

Metrology and Visualization of Potholes using the Microsoft Kinect Sensor

I. Moazzam, K. Kamal, S. Mathavan, S. Usman, M. Rahman

Abstract— Pavement distress and wear detection is of prime importance in transportation engineering. Due to degradation, potholes and different types of cracks are formed and they have to be detected and repaired in due course. Estimating the amount of filler material that is needed to fill a pothole is of great interest to prevent any shortage or excess, thereby wastage, of filler material that usually has to be transported from a different location. Metrological and visualization properties of a pothole play an important role in this regard. Using a low-cost Kinect sensor, the pavement depth images are collected from concrete and asphalt roads. Meshes are generated for better visualization of potholes. Area of pothole is analyzed with respect to depth. The approximate volume of pothole is calculated using trapezoidal rule on area-depth curves through pavement image analysis. In addition pothole area, length, and width are estimated. The paper also proposes a methodology to characterize potholes.

I. INTRODUCTION

Potholes are a significant feature of many parts of the highway network and are an irritation and nuisance to road users and highway maintenance staff alike. These localized failed areas also reduce ride quality and potentially create a dangerous driving condition. Various methods have been proposed so far, in order to detect pothole and also to characterize in terms of their shape, size, depth and volume. This is important to evaluate the extent of this distress, so that an appropriate maintenance measure can be taken.

In addition to manual measurements, vibration sensing, image and video analysis, and laser based techniques have been extensively used in practice. Techniques such as taking manual measurements are labor intensive, less accurate and subjective processes. On the other hand, vehicle vibration based measurement is economical but again not capable of providing either any volumetric measurement. Laser based methods are precise but expensive in terms of hardware requirements, data storage and processing equipment. Machine and industrial vision cameras are expensive and require proper lighting arrangements. Moreover, stereo-vision that is often proposed for 3D depth calculation has the disadvantage of its own that it cannot be used in low and no light conditions. However, the use of infrared technology based Kinect sensor for this purpose is still a novel idea. Moreover, it is cost effective as compared to industrial

cameras. The proposed method provides a low-cost alternative for the 3D analysis of pavement distress images. As compared to stereo-vision, in which 3D coordinates are calculated from two images, 3D imaging with Kinect sensor has the advantage that fewer calculations are required. As it provides direct depth measurements, therefore, need for computing power is drastically reduced.

II. PREVIOUS WORKS

Eriksson et al. [1] studied mobile sensing of roads to monitor and report any potholes. Accelerometer and GPS are used to detect and locate potholes respectively. Cars give detections which are fed to a central server to analyze and determine the pothole needed urgent repairing.

Koch et al. [2] studied vision tracking of potholes of pavement for road surveys. They tried pothole detection using video sequences. The texture of potholes is compared with a reference texture of pavement to detect it. They used a kernel based tracking of pothole. The pothole is detected first and then it is tracked. Matlab's image process toolbox was utilized for data processing. This technique gives the number of potholes detected in a recorded video.

Rajab et al. [3] studied pavement potholes and evaluated their area through image processing. They used curve fitting on points of pothole in 2D images. Yao et al. [4] used the second order moment operator on pavement surface images and calculated major axis, minor axis and orientation of potholes.

Youquan et al. [5] performed pothole detection using three dimensional projections. A line LED and camera sensors were used. The LED band light gives different behavior on pothole with respect to smooth surface. After binarization and initial processing, pothole was detected efficiently.

Joubert et al. [6] deployed GPS, Kinect, and a USB camera for pothole localization and data collection. GPS is used to locate the potholes. Pothole width is calculated manually using Kinect images and edges of potholes are detected from camera video sequence. Salari et al. [7] used stereo vision for pavement distress evaluation. They reconstructed the road surface and aimed to calculate severity of distress in future. Cruz et al. [8] surveyed the Kinect sensor and its application in robotics, games, and in natural interfaces, etc and conveyed important information about it.

III. KINECT SENSOR

Kinect is a low-cost imaging sensor, which has found its usage mainly in the areas of gaming, robotics, robot navigation, and obstacle avoidance. Its use has also been reported in object tracking. As the sensor also gives depth in

I. Moazzam, K. Kamal and S. Usman are with the National University of Sciences and Technology, Islamabad, Pakistan (phone: +92-323-6786453; e-mail: engr_sims@yahoo.com).

S. Mathavan and M. Rahman are with the School of Architecture, Design and the Built Environment, Nottingham Trent University, Burton Street, Nottingham NG1 4BU, UK.

addition to the RGB image, so it is very efficient in determining the location of object [9-11]. In addition to the RGB camera, it also consists of an IR sensor or camera that is used to measure the depth. The IR camera operates at 30 Hz frequency with the image size of 640x480 pixels. Depth images of resolution 1280x1024 pixels can also be taken through Kinect at the rate of 10 Hz. The field of view is 58 degrees horizontal, 45 degrees vertical, and 70 degrees diagonal. The reported range of operation is 0.8 to 3.5 meters [8]. However, Microsoft officially claims that the depth range is between 800 mm to 4000 mm. The camera also possesses the capability to switch to the near mode operation that enables the depth range of camera between 0 mm to 3000 mm [12]. It also has a tilt motor, an accelerometer, and microphones. Both the depth and RGB images, originally, may contain some noise. To avoid this, any of the techniques can be used such as, Average, Gaussian, or Median filtering. Some commercial and open source software for image and video acquisition through the Kinect sensor are OpenNI, Open Kinect, MicrosoftKinect for Windows SDK etc. The next section provides the details of experiment for pothole imaging using the Kinect sensor.

IV. EXPERIMENTATION

For analysis and evaluation, potholes were imaged in the NUST College of E&ME Rawalpindi, Pakistan, using the Kinect sensor in an evening between 4 to 5 pm. Image acquisition was done using the OpenKinect software in the Ubuntu Linux environment. Fig.1 shows the experimental setup. The metric (mm) depth images are used for further processing. Matlab is used as the processing environment.



Figure 13. Experimental Setup

Figure 2 is a depth image taken from the Kinect sensor. A depth image from a Kinect sensor is a two-dimensional array of pixels and each location of pixel (x, y) stores depth values in millimeters sensed by the IR sensor. All the values of depth image give distances in millimeters at each pixel ranging from 0 to 2047. Higher values at pixels represent the deeper points into the pavement surface.

Figure 3 is the corresponding RGB image of the same pothole from the RGB camera of the Kinect Sensor.

Kinect gives images of dimension 640x480 pixels. Using Matlab, the area of interest is then cropped to 540x380 pixels.

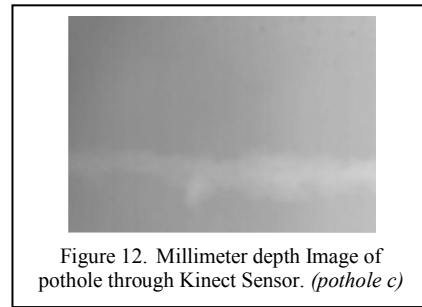


Figure 12. Millimeter depth Image of pothole through Kinect Sensor. (pothole c)

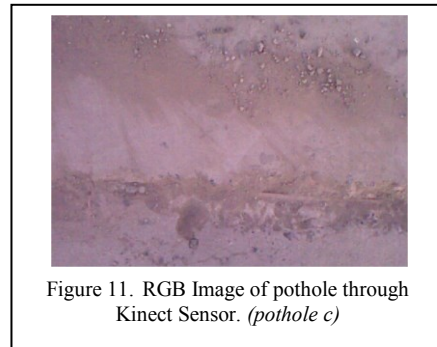


Figure 11. RGB Image of pothole through Kinect Sensor. (pothole c)

V. ALGORITHM

The images are taken with Kinect sensor held approximately at 0.8 to 0.9 meters above the ground and imported into the Matlab environment for further processing. An extensive data processing algorithm is written in order to process and extract the metrological as well as characterization features of the pothole. The local minimum of each column is calculated and then subtracted from the column itself in order to extract the pothole from the rest of data. The minimum of each column in road surface depth below which the pothole starts.

The z-axis (i.e. the depth axis) is already in real world coordinate system (mm), whereas, x and y coordinates are represented as pixels. So, the x-axis and the y- axis are converted to the real world coordinate system (mm) using Kinect depth and its field of view using (1) and (2)[13].

$$W_x = n_x \times d \times \alpha \dots\dots(1)$$

$$W_y = n_y \times d \times \beta \dots\dots(2)$$

Where,

W_x = World coordinate in x direction

n_x = normalized coordinate values along x-axis ranging from 0 to 1

d = depth in mm

α = constant based on Kinect's field of view for x-axis = 1.12032

W_y = World coordinates in y direction

n_y = normalized coordinate values along y-axis ranging from 0 to 1

$$\beta = \text{constant based on Kinect's field of view for y-axis} \\ = 0.84024$$

Meshes of potholes are generated subsequently with different azimuths and elevations for better visualization of potholes in real world coordinates. Then, mean, standard deviation, and maximum depth of pothole are calculated using Matlab's built-in functions. For area calculation of pothole, depth images are converted to binary for every millimeter increment in depth. For each step, binary area is calculated using Matlab built in function that gives number of *on* pixels. Final area at certain depth is calculated by multiplying binary area at that depth level and area of one pixel in world coordinates at that particular depth. Pixel area at certain depth is calculated from pixel length and width by triangulation method by using the law of cosines and the field of view of Kinect.

Area vs. depth curves are plotted to characterize potholes followed by the trapezoidal rule with unit spacing to calculate approximate volume. Contour plots (fig. 7) are also generated to see depth slicing where each color represent one depth level in millimeter with dark red for maximum and dark blue for minimum depth. The flowchart of the developed algorithm is shown in Fig. 4.

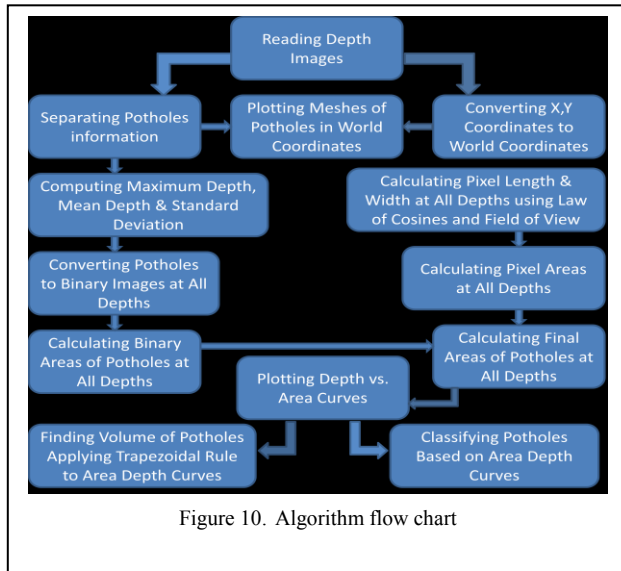


Figure 10. Algorithm flow chart

VI. RESULTS & ANALYSIS

Fig. 5 shows a 3D plot of *pothole c* with real-world coordinates in millimeters. The potholes are shown upside down, greater depths are the points with higher peaks in plot and meshes. Higher the peaks, higher the depth in 3D as well as in mesh plots afterwards.

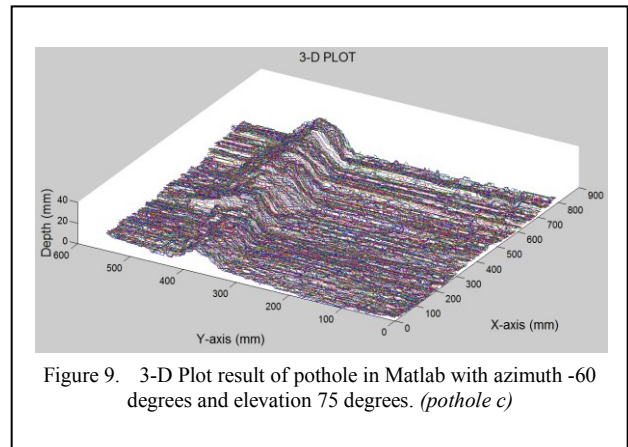


Figure 9. 3-D Plot result of pothole in Matlab with azimuth -60 degrees and elevation 75 degrees. (*pothole c*)

For better visualization mesh plots with normalized depth are generated.

The x and y coordinates of meshes are in real world coordinates(mm) while the z or depth axis is showing normalized real world double precision values from 0 to 1.

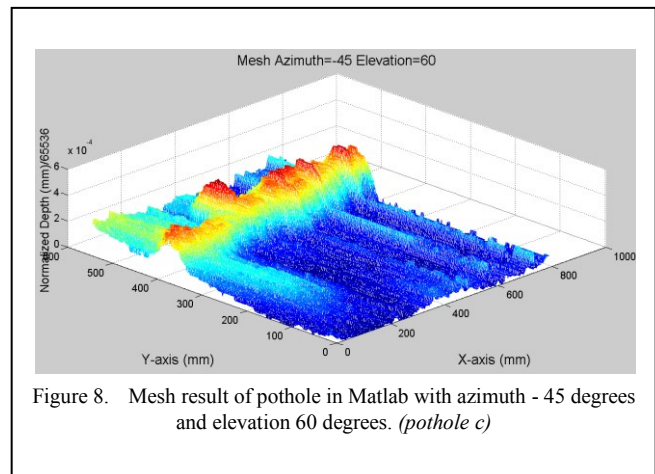
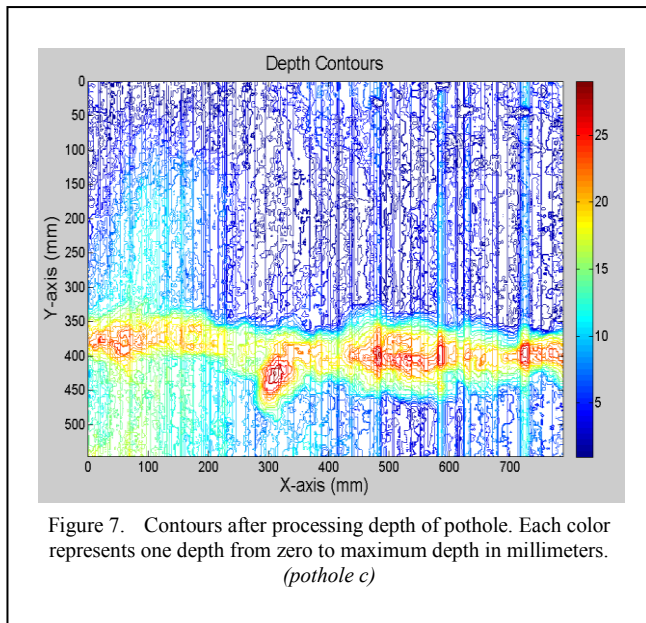


Figure 8. Mesh result of pothole in Matlab with azimuth - 45 degrees and elevation 60 degrees. (*pothole c*)

Fig. 6 shows the mesh of *pothole c*. It is clear from the figure that the points in dark blue color are the points closer to the road surface and the points in dark red color are the maximum depth level of the pothole. The rest of the colors are showing depths in between, and can be read by multiplying the value by 2^{16} . Fig. 7 shows the contour plot of the same pothole. Again, the dark blue regions show the points that are closer to surface, whereas, the dark red regions show the deepest points of the pothole, here again depth can be read from color bar.



Binary images are used to calculate areas at all depths. The on or white pixels show the depth of pothole below certain depth as shown in Fig. 8.

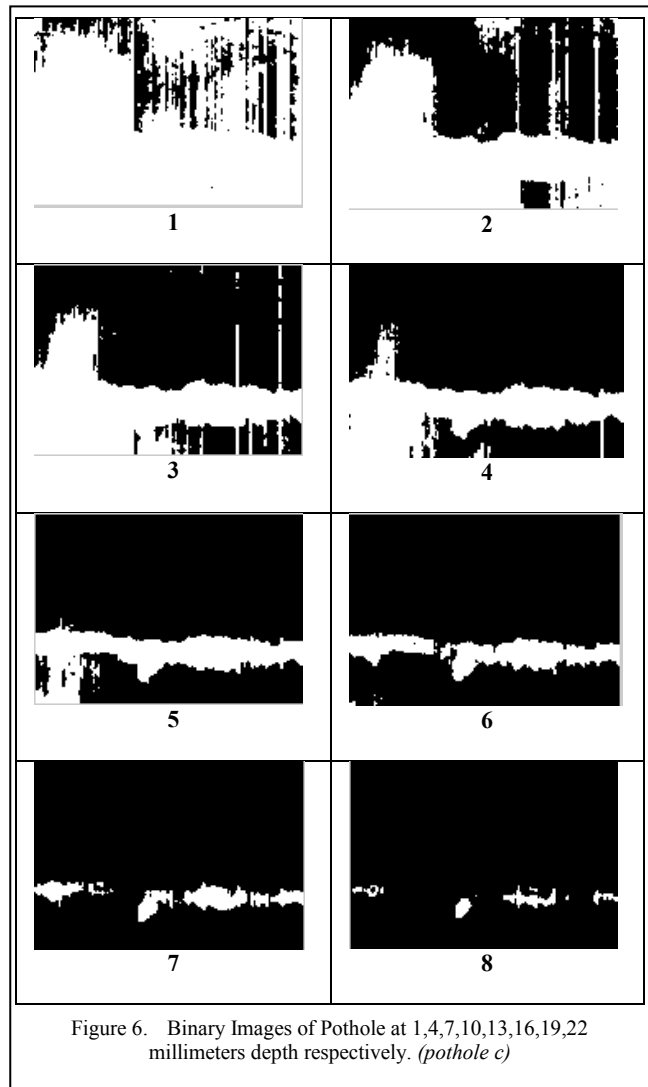
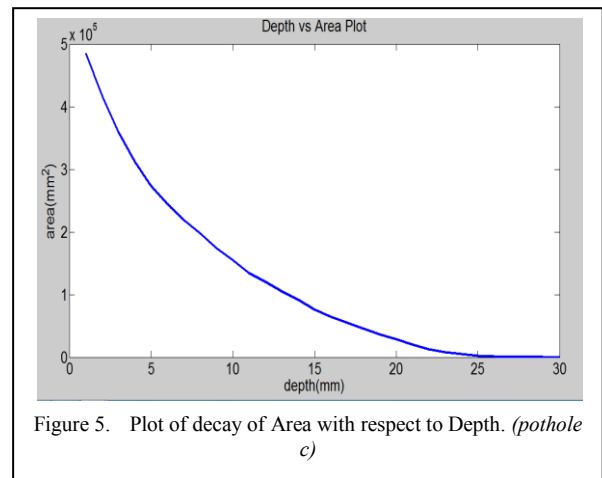


Fig. 9 shows the area verses depth plot. It shows how the area of pothole is changing with depth.



Second example is shown for more clarification of results.

Results of potholes *a* and *c* are detailed explicitly first and then with all selected 8 potholes.

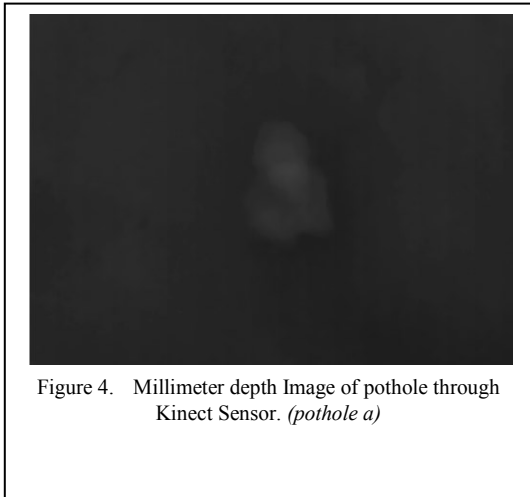


Figure 4. Millimeter depth Image of pothole through Kinect Sensor. (*pothole a*)

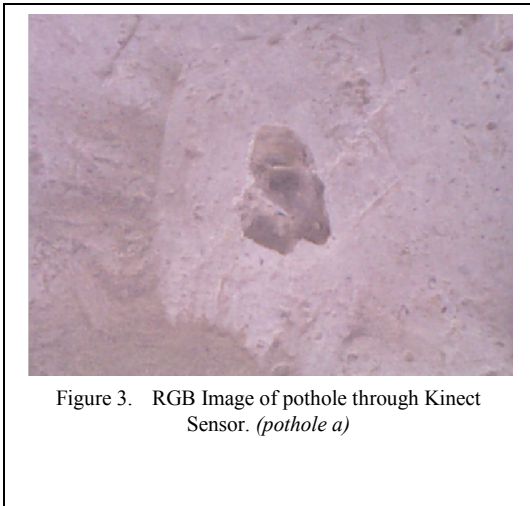


Figure 3. RGB Image of pothole through Kinect Sensor. (*pothole a*)

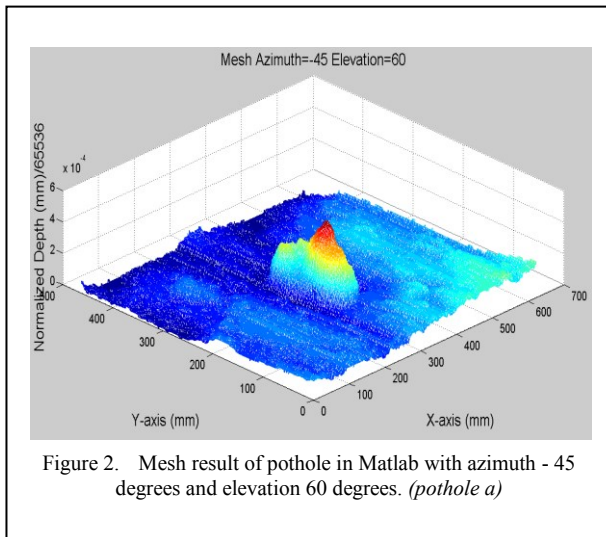


Figure 2. Mesh result of pothole in Matlab with azimuth - 45 degrees and elevation 60 degrees. (*pothole a*)

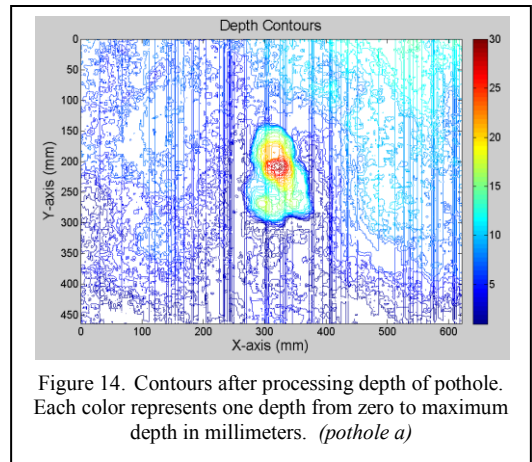


Figure 14. Contours after processing depth of pothole. Each color represents one depth from zero to maximum depth in millimeters. (*pothole a*)

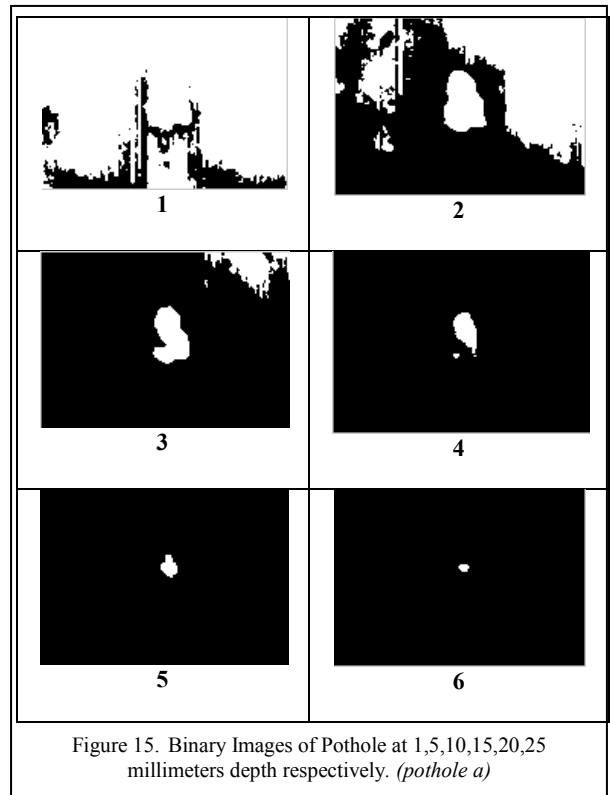


Figure 15. Binary Images of Pothole at 1,5,10,15,20,25 millimeters depth respectively. (*pothole a*)

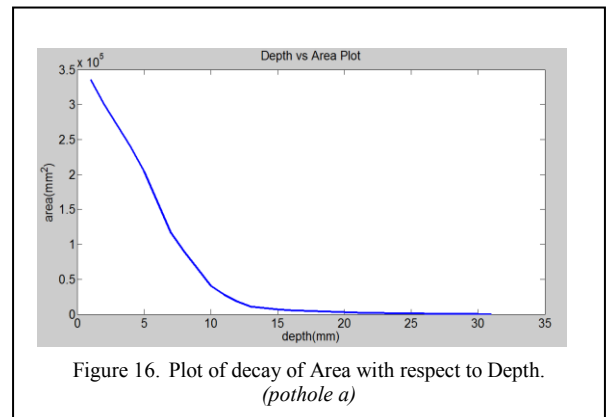


Figure 16. Plot of decay of Area with respect to Depth. (*pothole a*)

Eight different potholes are selected for results and analysis and their details are shown in fig 16 and 17.

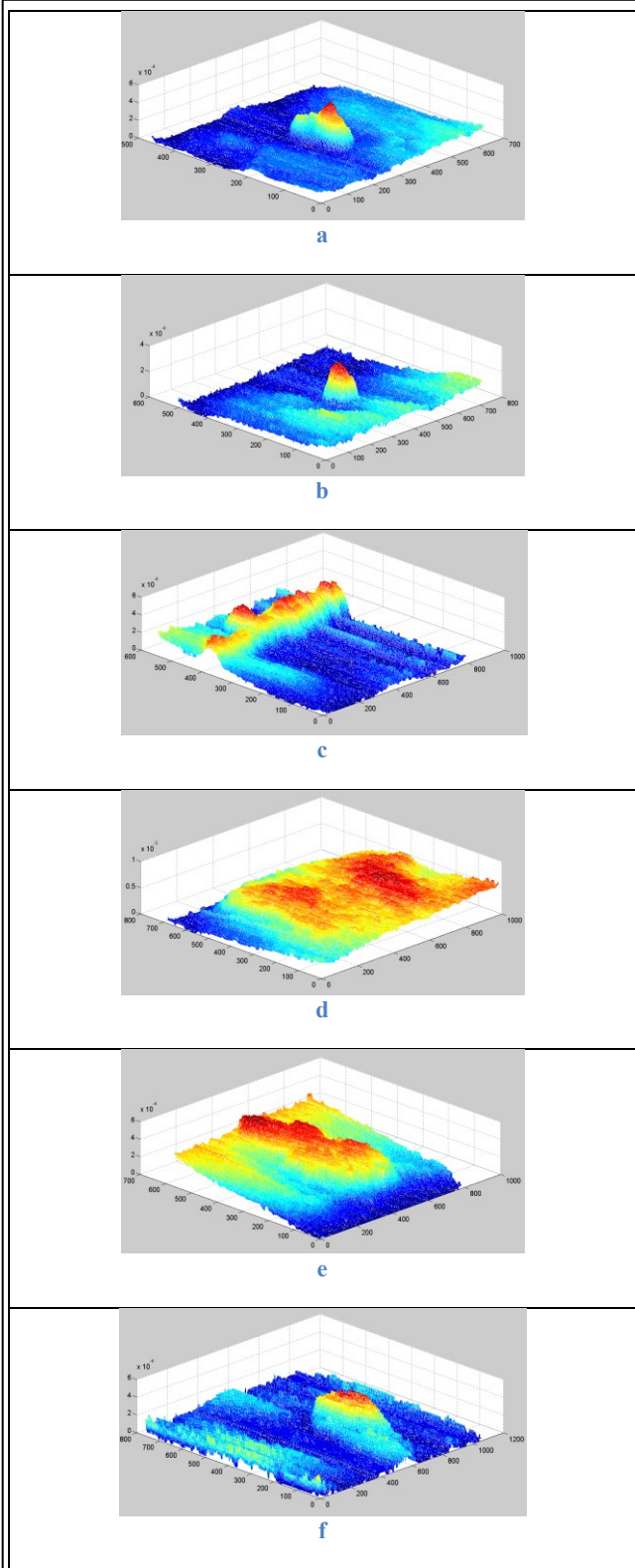


Figure 17. Mesh results of pothole in Matlab with azimuth - 45 degrees and elevation 60 degrees.

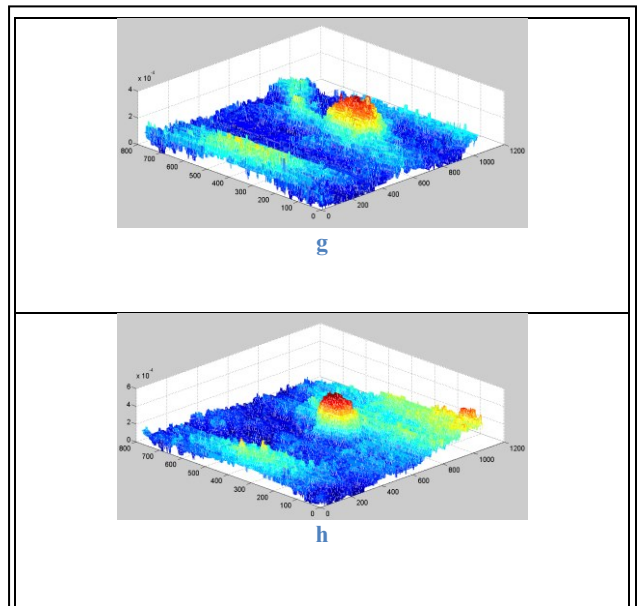


Figure 18. Mesh results of pothole in Matlab with azimuth - 45 degrees and elevation 60 degrees.

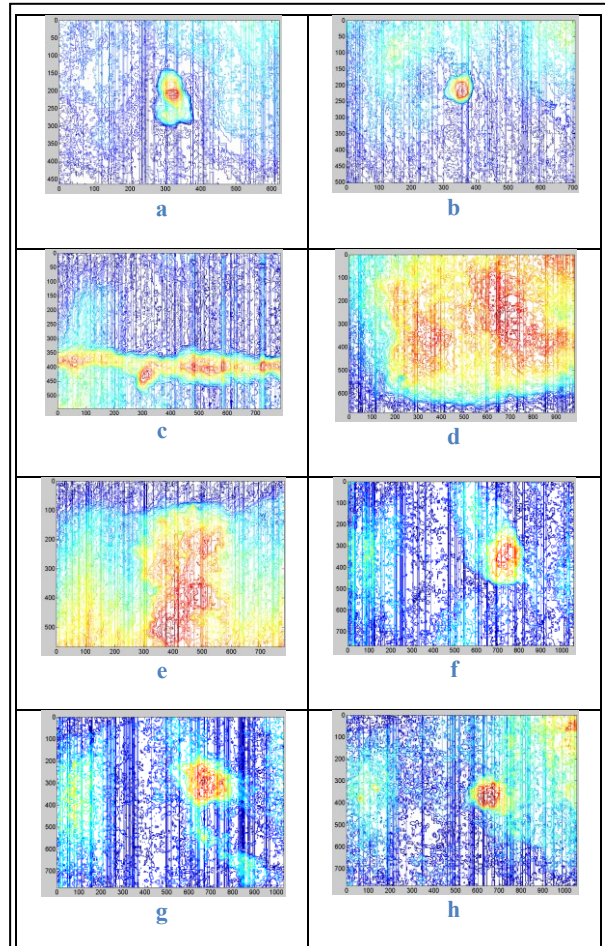


Figure 19. Contours after processing depth of pothole.

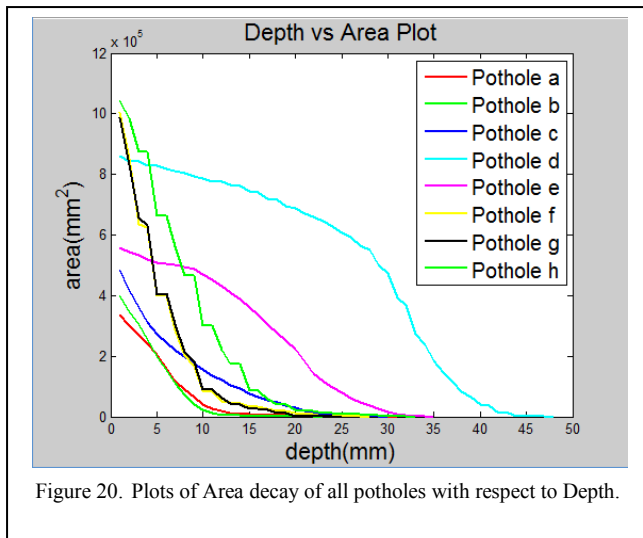


Figure 20. Plots of Area decay of all potholes with respect to Depth.

The plot of area decay with respect to depth gives some properties and classification of potholes (Fig. 19). The end of each curve on x or depth axis tells us that how much deep is that pothole. A prominent feature of the curves is that they all are monotonically decreasing. This condition holds true for any distress measured by this 3D imaging set up.

Based on these curves shown in Fig. 19 potholes can be characterized into 3 types. The first type has a squared decay. Potholes like pothole *a*, *b*, *f*, *g* and *h* whose area decrease almost 4 times, when the depth is halved, are conical in shape, approximately. The second type is the longitudinal pothole with two times area decay like pothole *c*. This is almost valley-shaped. The final type is cube-like. Potholes *d* and *e* whose area do not decrease too much initially and decays very quickly towards the bottom belong to this category.

Table 1 list out some of the metrological parameters of the 8 potholes shown in Fig.16 and Fig.17. Approximate volume is calculated by applying trapezoidal rule with unit spacing in the area-depth curves (Fig. 19). This volume includes surface roughness also.

The trapezoidal rule is given by (3).

$$\int_a^b f(x)dx \approx (b-a) \frac{f(a)+f(b)}{2} \dots\dots\dots(3)$$

The “side of cube” parameter (Table 1) tells us that if a perfect cube is made out of that volume then what will be the size of sides of that cube. The mean depth and the “side of cube” parameters demonstrate the size of pothole.

The pothole boundary is detected from binary images and region properties are calculated. These properties provide different metrological parameters of pothole like major axis and minor axis, centroid, eccentricity, orientation and perimeter, as listed in Table. 1. Major and minor axes give the geometrical feature of pothole. These features give an idea about the approximate length and width of the pothole respectively.

TABLE 1. POTHOLE FEATURE TABLE											
Pot-hole	Mean Depth (mm)	Standard deviation Depth (mm)	Max. Depth (mm)	Approx. Volume (cm³)	Side of Cube (cm)	Major Axis Length (mm)	Minor Axis Length (mm)	Centroid (mm,mm)	Eccentricity	Orientation (degree)	Perimeter (mm)
a	5.89	3.9	31	1760	12.07	182.45	112.60	375.40, 248.72	0.78	-81.04	420.91
b	4.97	3.2	23	1742	12.03	95.92	83.34	368.64, 213.76	0.49	50.72	251.76
c	7.16	6.2	30	3405	15.04	850.44	185.15	290.17, 390.59	0.97	2.89	2705.1
d	26.72	10.9	48	23030	28.45	658.72	458.18	432.21, 204.95	0.71	5.61	3298.1
e	16.51	8.0	35	9095	20.87	424.42	300.35	436.40, 347.09	0.70	-83.10	2475.1
f	5.42	4.1	28	4543	16.56	167.19	105.19	507.67, 236.23	0.77	86.49	686.90
g	5.46	4.0	25	4549	16.56	144.87	118.46	473.98, 197.29	0.57	-35.39	711.83
h	8.28	5.3	33	7693	19.74	165.96	126.82	478.10, 239.98	0.64	-19.7	1051.6

Centroid provides us the information regarding the geometrical centre of pothole. The Eccentricity is again a geometrical descriptor that provides us the information regarding the shape of the pothole. For a perfectly circular geometry, the value of eccentricity should be zero; however, we can say that potholes with eccentricity values closer to zero are circular, whereas for potholes having eccentricity values closer to 1 are longitudinal or elliptical in shape. Orientation provides the measure of tilt of the major axis of pothole in degrees with respect to x-axis ranging from -90 to 90. The metrological entities in table 1 are in error of approximately ± 15 percent compared to actual values. Further improvement in error rate is subject of future work.

VII. CONCLUSION AND FUTURE WORK

The Kinect sensor shows a promising future for pavement visualization and metrological analysis of potholes. Different parametric calculations can be easily and efficiently done on the images acquired by this sensor. It gives us more detailed data of pavement distress as compared to simple vision technique. This method is better than the stereo vision as depth measured by IR camera is readily available. It is also cheaper as compared to lasers.

The future works will involve the improvement in technique for volumetric measurement of potholes using tetrahedral mesh analysis. In addition, this research also aims to incorporate the analysis of Kinect accuracy through some transparent or slightly opaque medium such as water, as in rainy days, most of the potholes are filled with water.

From the metrological perspective, efforts will be made to accurately, and automatically, extract the edges of a given potholes. Distress edge determination is a contentious area within the research community and here it is aimed to make use of road standards and metrological norms to form a unified methodology to identify pothole edges. The same method will then be applied to other road distresses.

REFERENCES

1. J. Eriksson, L. Girod and B. Hull, "The Pothole Patrol: Using a Mobile Sensor Network for Road Surface Monitoring."
2. C. Koch and I. Brilakis, "Improving Pothole Recognition through Vision Tracking for Automated Pavement Assessment."
3. M. I. Rajab, M. H. Alawi, M. A. Saif, "Application of Image Processing to Measure Road Distresses," WSEAS Transactions on Information Science & Applications., Issue 1, Volume 5, January 2008.
4. X. Yao, M. Yao and B. Xu, "Automated Detection and Identification of Area-based Distress in Concrete Pavements," 7th International Conference on Managing Pavement Assets, 2008.
5. H. Youquan, W. Jian, Q. Hanxing, Z. Wei and X. Jianfang, "A Research of Pavement Potholes Detection Based on Three-Dimensional Projection Transformation," 4th International Congress on Image and Signal Processing, 2011.
6. D. Joubert, A. Tyatyantsi, J. Mphahlele and V. Manchidi, "Pothole Tagging System," 4th Robotics and Mechatronics Conference of South Africa (RobMech 2011), CSIR International Conference Centre, Pretoria, 23-25 November 2011.
7. E. Salari and E. Chou, "Pavement Distress Evaluation Using 3D Depth Information from Stereo Vision", Department of Electrical Engineering and Computer Science, The University of Toledo.
8. L. Cruz, D. Lucio, L. Velho, "Kinect and RGBD Images: Challenges and Applications,".

9. R. A. El-laithy, J. Huang and M. Yeh, "Study on the use of Microsoft Kinect for robotics applications" ,Position Location and Navigation Symposium (PLANS), 2012 IEEE/ION, General Topics for Engineers (Math, Science & Engineering), pp. 1280-1288, 2012.
10. D. S. O. Correa, D. F. Sciotti, M.G. Prado, D. O. Sales, D. F. Wolf and F. S. Osono, "Mobile Robots Navigation in Indoor Environments Using Kinect Sensor", Critical Embedded Systems (CBSEC), 2012 Second Brazilian Conference on Computing & Processing (Hardware/Software), pp. 36-41, 2012
11. P. Rakprayoon, M. Ruchanurucks and A. Coundoul, "Kinect-based obstacle detection for manipulator", System Integration (SII), 2011 IEEE/SICE International Symposium on Robotics & Control Systems., pp. 68 – 73, 2011.
12. <http://msdn.microsoft.com/en-us/library/hh438998.aspx>.
13. <http://qa.social.msdn.microsoft.com/Forums/en-US/kinectsdknuapi/thread/e53a4ba7-2522-407f-9d60-86e6fc5f89dc>